Lasers in Surgery and Medicine 25:1–7 (1999)

Free Electron Laser Infrared Wavelength Specificity for Cutaneous Contraction

Darrel L. Ellis, MD,[1]* Noah K. Weisberg, MD,[1] June S. Chen, MD,[1]
George P. Stricklin, MD, Ph.D,[1] and Lou Reinisch, PhD[2]

[1]Department of Medicine, Division of Dermatology, Vanderbilt University and Nashville Veterans Affairs Medical Centers, Tennessee 37232-5227
[2]Department of Otolaryngology, Vanderbilt University Medical Center, Nashville, Tennessee, USA 37232-2559

Background and Objective: **Short pulsed and scanned CO_2 lasers that target water molecules are currently used for cutaneous resurfacing. These CO_2 resurfacing lasers produce acute cutaneous contraction, which can be quantitated as a measure of the laser's effect. We postulated that targeting the vibrational and rotational modes of proteins with specific infrared laser wavelengths might be more effective at inducing cutaneous contraction than the CO_2 resurfacing lasers.**
Study Design/Materials and Methods: **The Vanderbilt University Free Electron Laser (FEL) was used at wavelengths between 6.0–8.6 μm. The cutaneous contraction and histologic thermal damage observed was compared to that seen with a scanned CO_2 resurfacing laser.**
Results: **Peaks of cutaneous contraction at 7.2–7.4 and 7.6–7.7 μm were found, which were three-fold more efficient at producing cutaneous contraction than the 10.6 μm CO_2 laser. The 7.2 μm wavelength is associated with the CH bend of C–CH_3, 7.4 μm to the CH bend of O=C–CH_3, 7.6 μm to the C–C–C stretch, and 7.7 μm to the amide III (C–N–H) absorption band for proteins. Using light microscopy, an approximately 40 μm denaturation zone of dermal collagen was found at all FEL wavelengths tested, regardless of the effectiveness of cutaneous contraction.**
Conclusion: **The mechanism of action of these infrared wavelengths on cutaneous contraction is unknown, but appears to be independent of the amount of collagen denatured as observed by light microscopy. Infrared lasers such as the FEL that target vibrational and rotational modes of proteins therefore hold promise for cutaneous application at selected wavelengths. Lasers Surg. Med. 25:1–7, 1999.** **© 1999 Wiley-Liss, Inc.**

Key words: absorption; collagen; resurfacing

INTRODUCTION

CO_2 lasers with short, high energy pulses or scanned laser systems have been used for resurfacing procedures such as treating facial rhytides [1–6]. The CO_2 laser (10.6 μm wavelength) produces cutaneous thermal heating primarily through interaction with water molecules [7]. Water is vaporized by the laser energy, leading to the tissue ablation seen with CO_2 laser resurfacing. The mechanism of action of these CO_2 cutaneous

Contract grant sponsor: Department of Defense Medical Free Electron Laser Program, Office of Naval Research (to DLE, JSC); Contract grant number: N00014-94-1023; Contract grant sponsor: National Institutes of Health; Contract grant number: P30AR41943.

June S. Chen is Free Electron Laser Fellow, Vanderbilt University and Nashville Veterans Affairs Medical Centers.

*Correspondence to: Darrel L. Ellis, 3900 The Vanderbilt Clinic, Nashville, TN 37232-5227.
E-mail: Darrel.Ellis@mcmail.Vanderbilt.edu

Accepted 20 January 1999

resurfacing lasers has not been completely explained, but appears to encompass elements of tissue contraction secondary to thermal denaturation of collagen (acutely), [8] and wound healing (chronically). How much each of these processes contributes to the final clinical result of resurfacing is currently the subject of much debate. For the purposes of testing multiple infrared wavelengths, requiring multiple assay points, we chose to focus on the acute process of tissue contraction for these experiments.

The Vanderbilt University Free Electron Laser (FEL) is an infrared laser that may be tuned to infrared wavelengths between 2–9 μm. This variety of available FEL wavelengths allows the study of laser irradiation of tissue with energies corresponding to the vibrational and rotational modes of proteins, proteoglycans, lipids, or water. The FEL pulse structure consists of picosecond micropulses separated by 350 psec, with about 17,000 micropulses per 4–6 μsec macropulse [9]. The macropulses repeat at 20 or 30 Hz. Although the FEL is a research laser that is restricted by its size and expense to use in limited institutions, concepts that can be tested with this infrared laser may later be used in commercial medical lasers for therapy.

We hypothesized that irradiation of cutaneous tissue with specific wavelengths of infrared laser energy that were targeted to dermal protein absorption would result in more efficient cutaneous contraction than would nonspecific water absorption. To test this hypothesis, we used Fourier-transform infrared spectroscopy to define epidermal and dermal absorption peaks of human skin. The FEL was then used to study the interaction of infrared laser energy with human skin at these absorption peaks. Previous work with the FEL found that radiation with energy at the amide II protein absorption band (6.45 μm) leads to precise incisional wounds with tissue ablation characterized by minimal collateral thermal damage [9]. This wavelength was therefore of particular interest, and tested in our resurfacing system. Human skin was utilized for these studies in an experimental cutaneous contraction model we have previously used for CO_2 resurfacing lasers [8]. We measured acute contraction of the skin, and compared the collagen thermal damage at the different wavelengths by using histology with collagen staining by Gomori's trichrome.

MATERIALS AND METHODS

Tissue

Human skin samples obtained with the consent of the Vanderbilt University Institutional Review Board as excess tissue from reduction mammoplasties or abdominoplasties were used for all experiments. The tissue was stored on saline moistened gauze pads at 4°C and utilized within 48 hours of harvest, or double wrapped in aluminum foil, sealed in a ziplock bag, frozen at –20°C, and utilized within two months. A plastic template was used to cut (2.0 × 0.5) cm^2 specimens, which were used for the experiments.

Fourier Transform Infrared Spectroscopy

Absorption peaks were determined for human epidermal and dermal tissue by studying a (3 × 1) cm^2 sample of human facial skin that was obtained as excess tissue from a rhytidectomy, wrapped in saline soaked gauze, and transported on ice for immediate use in the assay. The epidermal absorption pattern was measured on the epidermis side of the intact skin sample. The dermal absorption pattern was measured after sharp dissection of the epidermis and confirmed by measuring the spectrum on the underside of the sample, which had been defatted. Evaluation was done using an attenuated total reflection cell in a Fourier-Transform Infrared Spectrometer (Bruker Instruments, Inc., Billerica, MA).

Lasers

The Free Electron Laser (FEL) at Vanderbilt University was utilized at wavelengths ranging from 6.0 to 8.6 μm. The laser was operated at 20 Hz and from 25–37 mJ with a 4–6 μsec macropulse for the experiments. The laser beam was delivered with a Computer Assisted Surgical Technique (CAST) system designed by one of the authors [10]. Fifteen rows of 40 non-overlapping spots were used to deliver a grid covering a (1.6 × 0.7) cm^2 area. This grid provides a treatment area similar to that used with CO_2 resurfacing lasers. The minimum laser power was 25 mJ (25–37 mJ). This resulted in a minimum average fluence over the treated area of 7.2 J/cm^2, with a fluence of 12.7 J/cm^2 at each spot where the laser pulse was incident on the tissue. We tested the absorption peaks and selected flanking regions shown in Table 1 with the FEL to demonstrate the specificity of molecular absorption of infrared radiation by protein.

TABLE 1. Infrared Wavelengths Tested With the FEL and the Corresponding Molecular Absorption Bands

Wavelength (μm)	Protein absorption band
6.1	Amide I (C–N–H)
6.45	Amide II (C–N–H)
6.8	C–H bend of CH_2 or CH_3
7.0	COO^- asymmetry stretch
7.2	C–H bend of $C–CH_3$
7.4	C–H bend of $O=C–CH_3$
7.5	Control flanking region
7.6	C–C–C stretch
7.7	Amide III (C–N–H)
8.0	Control flanking region
8.1	C–N stretch
8.6	$(CH_3)CH$–stretch
10.6	CO_2 laser control

The FEL was compared to the Silk Touch® cutaneous resurfacing laser. The Sharplan Silk Touch (Allendale, NJ) 125 mm hand piece with a 3.4 mm (measured) spiral-scanned pattern was connected to a Sharplan 1060 CO_2 laser set at 8 W with a 200 msec repeated pulse at 1 Hz for a total of 1.6 J/pulse as previously published [8]. The handpiece was set to the "+" spot size. The fluence as measured here was 17.6 J/cm^2, whereas the manufacturer's stated fluence was 13.7 J/cm^2.

Operating Parameters

Tissue within a 1.6 × 0.7 cm^2 centrally placed grid on the 2.0 × 0.5 cm^2 strip of human skin was completely irradiated with non-overlapping CAST guided impulses for the FEL laser, or non-overlapping manually controlled impulses for the Silk Touch® laser. The pattern was slightly wider than the tissue to assure that the tissue was completely irradiated between the tattooed areas. Each tissue specimen received up to five laser passes. Following each pass, the irradiated region was debrided vigorously with a saline moistened cotton swab, then blotted dry prior to the next pass.

Tissue Shrinkage

Tissue shrinkage was evaluated by measuring the linear distance change between two centrally placed India ink tattoos, placed 1.2 cm apart. The tissue was digitally photographed prior to irradiation and subsequent to each laser pass and debridement. The digital photographs were taken at 25× magnification with an Ikegami MKC-301A video camera (Tokyo, Japan) mounted to the sideport of an OPHI surgical microscope with a 400 mm focal length lens (Zeiss, Germany). The camera was interfaced with the built-in video port of a MAC 840 AV microcomputer (Cupertino, CA). Distances were measured with Adobe Photoshop 2.0 (Mountainview, CA).

Data Evaluation

Each data point in Figure 2 represents at least three separate samples. The slope for each wavelength was evaluated by at least two complete experiments on separate days (six separate samples). Individual wavelengths results were plotted in relative length vs. Energy (J/cm^2). Different wavelengths were compared by plotting either (% Change in Length)/(J/cm^2) or (% Change in Length)/(Pass of the Laser).

Histology

Tissue specimens were fixed in 10% formalin, embedded in paraffin, sectioned, and stained with either hematoxylin and eosin or Gomori's trichrome stain for light microscopic evaluation. Analysis was performed with an Olympus Vanox AH-2 light microscope (Lake Success, NY). The depth of thermal denaturation was quantitated by using tissue morphometry measurements done with a Southern Micro Instruments planar morphometry software (Atlanta, GA). Histologic figures were made with digital images made with ProgRes 3008 (Kowtron Elektronik, Eching, Germany), with all images taken at 100×.

RESULTS

Fourier-transform infrared spectroscopy showed specific epidermal and dermal absorption. The spectroscopy results are shown in Figure 1. Figure 1a shows the epidermal absorption plotted vs. wavelength (μm). The OH stretch, amide II, carbonate, and amide III absorption bands are plotted as reference points. Major peaks of absorption are seen at 6.1, 6.45, 6.8, 7.25, 8.0, 8.6, 8.9, and 9.1 μm. Figure 1b shows the dermal absorption spectrum. Similar peaks of absorption are seen, although the peaks are higher in the dermis for 6.1 and 6.45 μm, and lower for 8.0 and 8.6 μm. These peaks of absorption as well as selected protein absorption bands were studied as shown in Table 1.

The results of the tissue contraction experiments for selected wavelengths are shown in Figure 2. The Silk Touch data were previously pub-

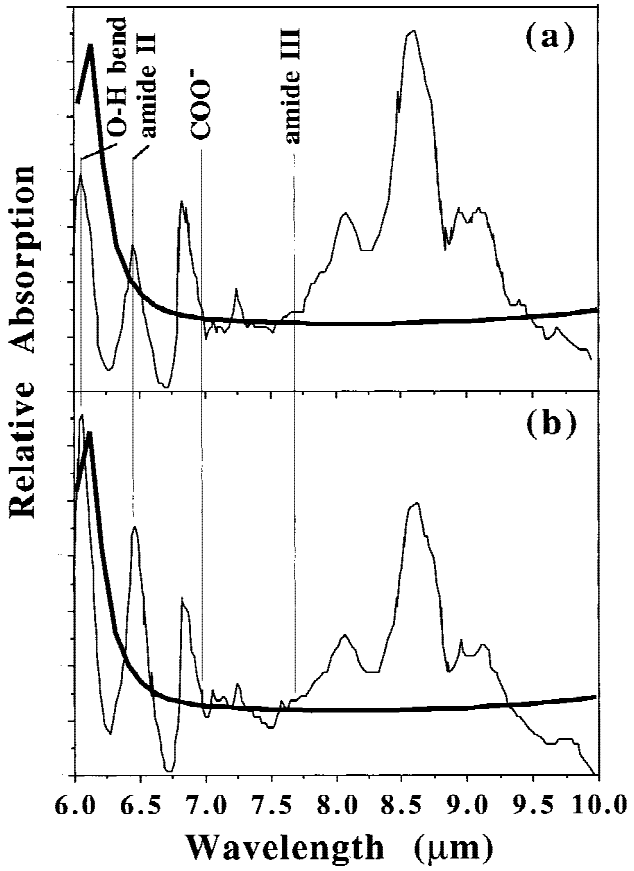

Fig. 1. Fourier-transform infrared spectroscopy of human skin (thin line) with H_2O plotted as a reference (thick line). Absorption is plotted vs. wavelength (μm). The O–H bend, amide II, COO^-, and amide III absorption bands are plotted as reference points. **(a)** Epidermal absorption spectrum. **(b):** Dermal absorption spectrum.

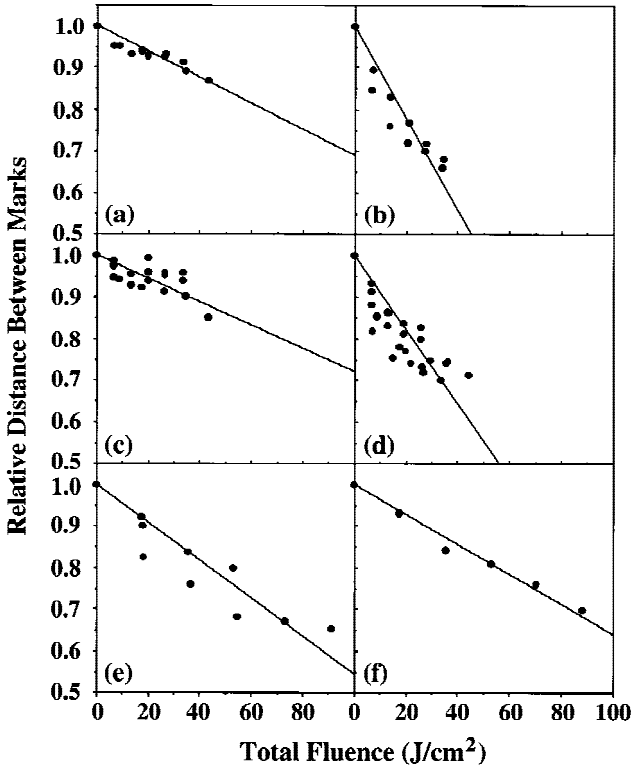

Fig. 2. Plots of relative lengths of the treated tissue measured by digital photography vs. the energy of the laser irradiation (J/cm^2). The steeper the slope of the line, the more shrinkage was observed. **(a)** 6.45 μm, **(b)** 7.4 μm, **(c)** 7.5 μm, **(d)** 7.7 μm, **(e)** 8.6 μm, **(f)** 10.6 μm (SilkTouch CO_2 Laser, from Gardner et al., 1996, included for comparison).

lished [8]. The relative length of the tissue measured by digital photography is plotted vs. the energy of the laser irradiation (J/cm^2). The energy of the laser irradiation data points increase incrementally in correspondence to the passes made with the laser over the tissue. Although there was considerable experimental scatter, the best fit of these data was a straight line in all cases. The slope of each line shows the shrinkage obtained at that wavelength. The wavelengths with the steeper slopes therefore had the best cutaneous contraction. To compare the tissue contraction obtained with different wavelengths of laser irradiation, the data are presented in two ways. The shrinkage related to fluence (% Change in Length)/(J/cm^2) was plotted vs. the wavelength (Fig. 3a) to show the efficiency of the energy at a given wavelength for producing contraction. The shrinkage related to pass of the laser (% Change in Length/Pass) was plotted vs. the wavelength (Fig. 3b) to show the efficiency of the laser per pass in producing contraction. This dual comparison was done because the shrinkage of tissue does not always increase linearly with increased fluence [11]. The best cutaneous contraction was observed at the 7.2–7.4 μm and 7.6–7.7 μm infrared laser wavelengths. Both of these wavelength bands exhibited much more % shrinkage per fluence used than the control CO_2 laser.

Gomori's trichrome stain was used to evaluate the thermal damage seen at all FEL wavelengths tested. Representative histologic results seen with FEL irradiation are shown in Figure 4. All photographs shown were done after laser pass number 3. This is typically the maximum number of passes used clinically for facial resurfacing. The depth of ablation extended into the upper reticular dermis in all samples. However, we had no way to reliably quantitate the depth of tissue ablated. Thermal denaturation was measured by the tincture change of collagen by using quantitative computer image analysis. Approximately

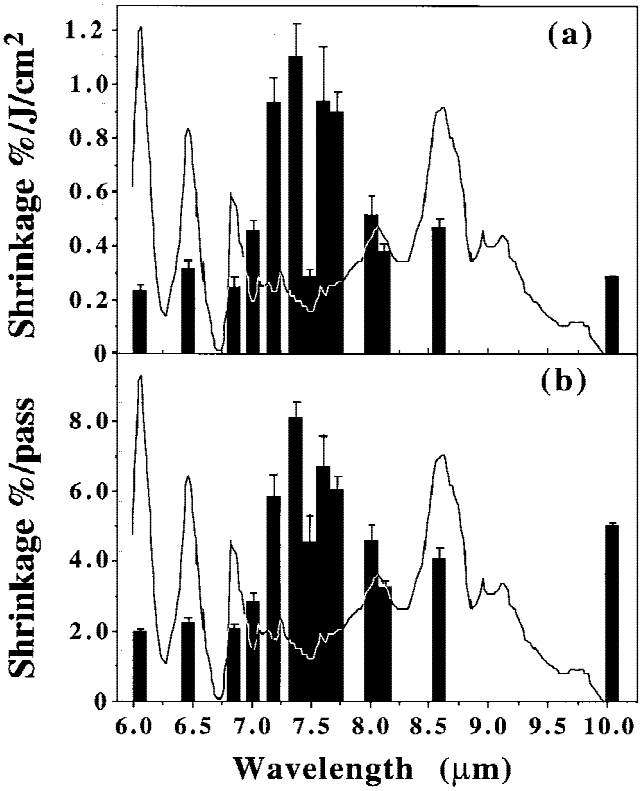

Fig. 3. Comparison of the cutaneous shrinkages obtained at different laser wavelengths. **(a)** Amount of shrinkage related to fluence (% Change in Length)/(J/cm^2) plotted vs. the wavelength tested (μm). **(b)** Amount of shrinkage related to the pass of the laser beam (% Change in Length)/(Pass) plotted vs. the wavelength tested (μm). Results are superimposed upon the epidermal Fourier-transform infrared spectroscopy data for purposes of orientation.

40 μm of thermal damage was measured at all FEL wavelengths tested.

DISCUSSION

Our studies with the FEL demonstrate that selected infrared irradiation wavelengths are better at inducing cutaneous contraction than the standard resurfacing CO_2 lasers. The two peaks for best cutaneous contraction were observed at 7.2–7.4 and 7.6–7.7 μm. The 7.2–7.4 μm peak encompasses the C–H bend of C–CH_3 at 7.2 μm and the C–H bend of O = C–CH_3 at 7.4 μm. The 7.6–7.7 μm peak includes the C–C–C stretch at 7.6 μm, and the amide III (C–N–H) absorption band at 7.7 μm. These results suggest that targeting selective protein absorption may provide better clinical effect for cutaneous resurfacing than targeting water absorption (CO_2 laser). We did not observe greater cutaneous contraction at 6.45 μm, although this protein absorption wavelength (amide II band) has been studied for laser ablation, and was used successfully for incisional wounds [9]. We assume the strong water absorption at 6.45 μm (the tail of the 6.1 μm water absorption band) probably competes with the amide II protein absorption and makes this band less effective for cutaneous contraction than the 7.2–7.4 and 7.6–7.7 μm bands.

Histology of the FEL treated tissue shows a thermal denaturation zone of approximately 40 μm at each wavelength tested as measured by Gomori's trichrome staining. Our histologic results were done on acutely injured in vitro tissue. The results in vivo may vary, and the depth of injury may be greater later in the time course (such as 24–48 hour postoperative). The observed 40 μm of thermal denaturation should provide adequate hemostasis in vivo, yet limit the collateral tissue damage. The FEL thermal denaturation zone of 40 μm compares favorably to the 50–100 μm denatured areas commonly seen with CO_2 resurfacing lasers in in vitro and in vivo studies [1,8,11,12]. In vivo studies may vary from in vitro studies. However, we have found similar results in previous studies with these techniques using CO_2 resurfacing lasers [11]. Thermal denaturation may be responsible for much of the morbidity of cutaneous laser resurfacing, such as hypertrophic scarring, pigmentary change, and persistent postoperative erythema [13]. Wavelengths such as 7.2–7.4 and 7.6–7.7 μm therefore need testing in vivo to see if less cutaneous side effects are observed.

Current theory of the mechanism of action of CO_2 resurfacing lasers attributes the acute clinical effect of shrinkage to collagen denaturation and contraction. This implies that a larger zone of collagen denaturation should produce greater clinical contraction. We saw large differences in clinical contraction with the same zone of thermal damage observed with light microscopy. This implies either collagen denaturation is not solely responsible for tissue contraction, or collagen denaturation is not the same at different wavelengths, although it may look similar with light microscopy.

Kirsch et al. [14] found by using three different resurfacing lasers that there was a zone of thickened collagen fibers, which was below the area of completely denatured collagen. They suggested that these collagen fibers had contracted linearly, and were responsible for the cutaneous shrinkage observed clinically. They found this

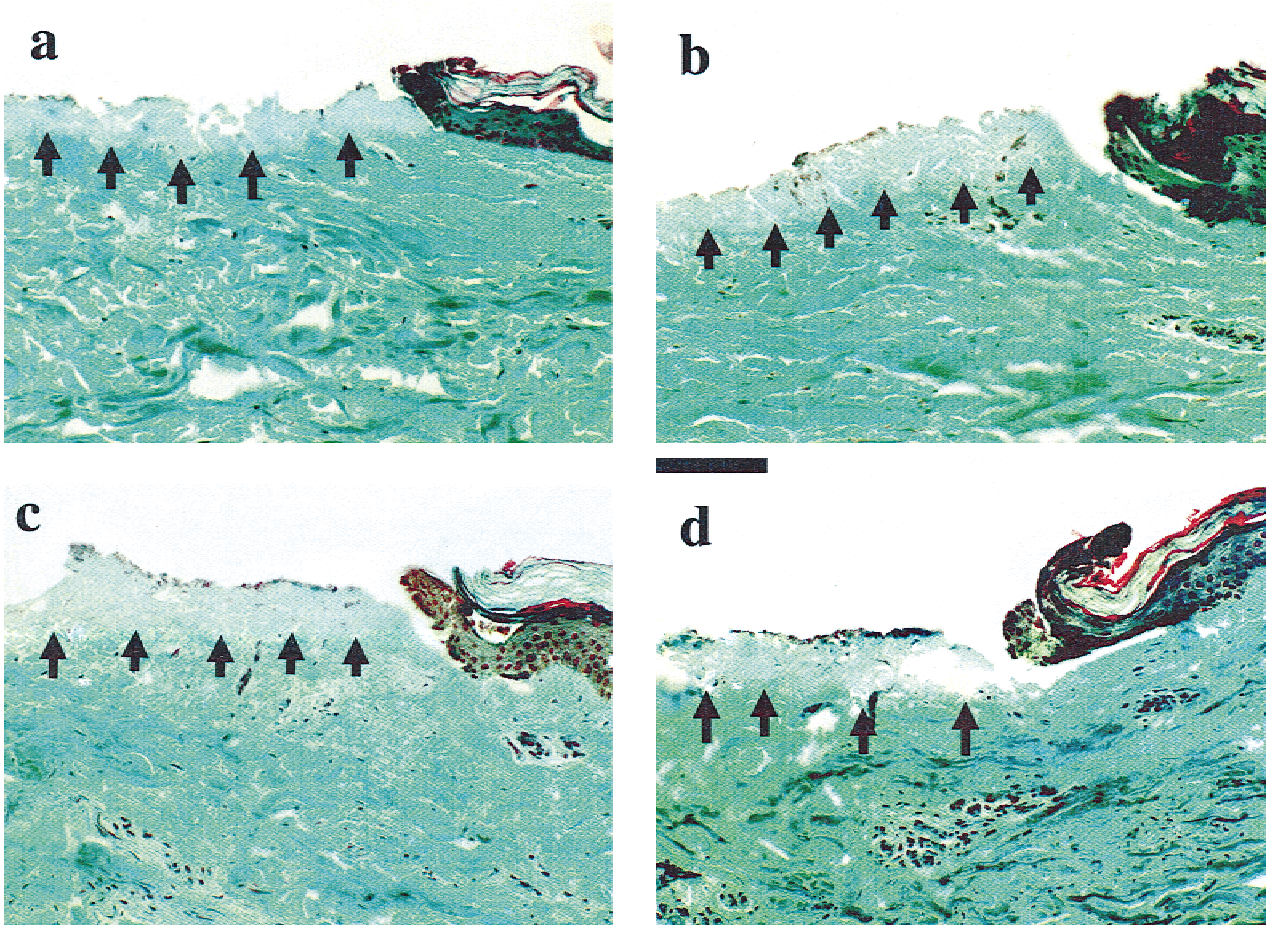

Fig. 4. Histology of human skin treated with the FEL, stained with Gomori's trichrome. **(a)** 7.00 μm, **(b)** 7.4 μm, **(c)** 7.5 μm, **(d)** 7.7 μm. All samples show approximately 40 μm of thermal denaturation as denoted by the tincture change of the dermis (arrows). All magnifications = 100×. Scale bar = 100 μm.

zone to be 9 and 15 μm for single- or double-laser passes for all of the CO_2 resurfacing lasers tested. This suggested that increased fluence leads to increased linear collagen fiber contraction. This zone was not distinguishable on light microscopy with hematoxylin-eosin staining, and was thought to be in the area characterized by tinctorial change. However, we observed variable amounts of contraction at different FEL wavelengths whereas the amount of thermal denaturation remained relatively constant. This suggests either the zones of contracted collagen fibrils may vary, although the light microscopy tinctorial change was the same, or other mechanisms of action may be involved in laser resurfacing, particularly when the molecular target is the vibrational mode of protein, and not water. Electron microscopy studies may help clarify this question.

In conclusion, we found two infrared energy bands (7.2–7.4 and 7.6–7.7 μm) that demonstrated increased cutaneous contraction relative to the fluences used or passes made when compared to the CO_2 resurfacing laser. This indicates that selective molecular targeting such as the protein vibrational modes at 7.2, 7.4, 7.6, and 7.7 μm with infrared lasers may provide more efficient resurfacing lasers. Selective molecular targeting may also allow less tissue irradiation and less thermal damage, with the possibility of reduced clinical morbidity. Because our data suggest that collagen denaturation may not be solely responsible for tissue contraction at the wavelengths we tested, further studies to clarify the mechanisms of laser cutaneous tissue interaction are clearly indicated.

ACKNOWLEDGEMENTS

The expert technical assistance of Lillian B. Nanney, Ph.D., and Mary McKissack is gratefully acknowledged.

REFERENCES

1. Chernoff G, Slatkine M, Zair E, Mead D. Silktouch: a new technology for resurfacing in aesthetic surgery. J Clin Laser Med and Surg 1995;13:97–100.
2. David LM, Sarne A, Unger WT. Rapid laser scanning for facial resurfacing. Dermatol Surg 1995;21:1031–1033.
3. Fitzpatrick RE, Goldman W, Satur NM, Tope WD. Pulsed carbon dioxide laser resurfacing of photoaged facial skin. Arch Dermatol 1996;132:395–402.
4. Lask G, Keller G, Lowe N, Gormley D. Laser skin resurfacing with the SilkTouch flashscanner for facial rhytides. Dermatol Surg 1995;21:1021–1024.
5. Lowe NJ, Lask G, Griffen ME, Maxwell A, Lowe P, Quilada F. Skin resurfacing with the ultrapulse carbon dioxide laser: observations on 100 patients. Dermatol Surg 1995;21:1025–1029.
6. Waldorf HA, Kauvar ANB, Geronemus RG. Skin resurfacing of fine to deep rhytides using a char-free carbon dioxide laser in 47 patients. Dermatol Surg 1995;21:940–946.
7. Hale GM, Querry MR. Optical constants of water in the 200-nm to 200-μm wavelength region. Applied Optics 1973;12:555–563.
8. Gardner ES, Reinisch L, Stricklin GP, Ellis DL. In vitro changes in non-facial human skin following CO_2 laser resurfacing: a comparison study. Lasers Surg Med 1996; 19:379–387.
9. Edwards G, Logan R, Copeland M, et al. Tissue ablation by a free-electron laser tuned to the amide II band. Nature 1994;371:416–419.
10. Reinisch L, Mendenhall M, Charous S, Ossoff RH. Computer-assisted surgical techniques using the Vanderbilt free electron laser. Laryngoscope 1994;104:1323–1329.
11. Weisberg NK, Kuo T, Torkian B, Reinisch L, and Ellis DL. Optimizing fluence and debridement effects on cutaneous resurfacing CO_2 laser surgery. Arch Dermatol 1998;134:1223–1228.
12. Kauvar ANB, Waldorf HA, Geronemus RG. A histopathological comparison of "charfree" carbon dioxide lasers. Dermatol Surg 1996;22:343–348.
13. Bernstein LJ, Kauvar ANB, Grossman MC, and Geronemus RG. The short- and long-term side effects of carbon dioxide laser resurfacing. Dermatol Surg 1997;23:519–525.
14. Kirsch KM, Zelickson BD, Zachary CB, and Tope WD. Ultrastructure of collagen thermally denatured by microsecond domain pulsed carbon dioxide laser. Arch Dermatol 1998;134:1255–1259.